Cephalopod Retinal Development Shows Vertebrate-like Mechanisms of Neurogenesis

Francesca Napoli*, Christina M. Daly*, Stephanie Neal, Kyle J. McCulloch, Alexandra Zaloga, Alicia Liu, Kristen M. Koenig

*These authors contributed equally to this work

John Harvard Distinguished Science Fellowship Program, Harvard University, Cambridge, MA 02138 USA.

Department of Organismic and Evolutionary Biology, Harvard University, Cambridge, MA 02138 USA

Email: kmkoenig@fas.harvard.edu

Abstract

Neurogenesis, the regulation of cellular proliferation and differentiation in the developing nervous system, is the process that underlies the diversity of size and cell type found in animal nervous systems. Our understanding of how this process has evolved is limited because of the lack of high resolution data and live-imaging methods across species. The retina is a classic model for the study of neurogenesis in vertebrates and live-imaging of the retina has shown that during development, progenitor cells are organized in a pseudostratified neuroepithelium and nuclei migrate in coordination with the cell cycle along the apicobasal axis of the cell, a process called interkinetic nuclear migration. Eventually cells delaminate and differentiate within the boundaries of the epithelium. This process has been considered unique to vertebrates and thought to be important in maintaining organization during the development of a complex nervous system. Coleoid cephalopods, including squid, cuttlefish and octopus, have the largest nervous system of any invertebrate and convergently-evolved camera-type eyes, making them a compelling comparative system to vertebrates. Here we have pioneered live-imaging techniques to show that the squid, *Doryteuthis pealeii*, displays cellular mechanisms during cephalopod retinal neurogenesis that are hallmarks of vertebrate processes. We find that retinal progenitor cells in the squid undergo interkinetic nuclear migration until they exit the cell cycle, we identify retinal organization corresponding to progenitor, post-mitotic and differentiated cells, and we find that Notch signaling regulates this process. With cephalopods and vertebrates having diverged 550 million years ago, these results suggest that mechanisms thought to be unique to vertebrates may be common to highly proliferative neurogenic primordia contributing to a large nervous system.

Introduction

Coleoid cephalopods (e.g. squid, cuttlefish and octopus) are charismatic invertebrates known for their expansive behavioral repertoire and large nervous system. One of the striking features of the cephalopod nervous system is their camera-type eyes, which are one of the most acute visual organs among animals (Gagnon et al., 2013; Packard, 1972). This complexity in cephalopods is independently evolved from similar features found in vertebrate species. Although vertebrates have been well studied, the developmental changes that underlie the evolution of large, complex nervous systems are not well understood. Observations in traditional model organisms show that diversity in nervous system size and functionality across animals is a product of diversity in developmental processes (Hartenstein & Stollewerk, 2015). We know that in some cases neurogenesis is highly regulated with invariant numbers of precursors with fixed lineages (i.e. *C. elegans*), and in others cell lineages are stochastic or plastic (i.e. the vertebrate retina) (Bertrand & Hobert, 2010; Zechner et al., 2020); (Hartenstein & Stollewerk, 2015). Live-imaging has changed our perspective on neurodifferentiation from a primarily genetic process to a cell biological process, defined by orchestrated cell behaviors and tissue architecture. However, *in vivo* observations of neurogenesis have been limited to vertebrates and *Drosophila*. To elucidate how changes in neurogenesis may contribute to the evolution of large and complex nervous systems, we sought to understand neurodifferentiation in the cephalopod. The visual system has proven to be a powerful context to learn fundamental aspects of neural development in vertebrates and *Drosophila* and therefore we have chosen to focus our investigations on retinal differentiation in the squid *Doryteuthis pealeii.*

The adult cephalopod retina is composed of two layers divided by the basal membrane (Figure 1A). Photoreceptor cell bodies are found posterior (further from the lens) to the basal membrane and support cells are found anterior (closer to the lens). The photoreceptor cells extend projections to the anterior of the retina to form the outer segment layer and extend axons out of the posterior retina to synapse directly on the optic lobe (Yamamoto et al., 1965; Young, 1974). During development, photoreceptor cell bodies are first identified behind the basal membrane at Arnold embryonic stage 27, and these cells are no longer proliferative (Arnold, 1965; Koenig et al., 2016). This is the earliest evidence of differentiation in the retina. The support cells, in the anterior of the retina, also extend processes into the outer segment (Yamamoto et al., 1965). Although the eye is functional at hatching, the support cells continue to incorporate BrdU (Koenig et al., 2016). The animal continues to grow post-hatching and proliferating support cells may include a long-term retinal stem cell population.

67 Previous observations from fixed tissue suggested that the cephalopod retinal primordium
68 is a pseudostratified epithelium, which is unusual for an invertebrate neurogenic tissue (Koenig
69 et al, 2016; (Koenig & Gross, 2020) (Figure 1A). This type of neuroepithelium is characteristic of
70 central nervous system development in vertebrates, including the retina (Taverna et al., 2014). A
71 pseudostratified epithelium is a monolayer composed of elongated cells with nuclei distributed
72 along the apicobasal axis. Cells in pseudostratified epithelia undergo nuclear movement
73 correlated with the cell cycle called interkinetic nuclear migration (Norden, 2017). This migration
74 is required for proper differentiation and organization in the developing vertebrate nervous system
75 (Strzyz et al., 2016). During nuclear migration, mitosis occurs on the apical surface and in
76 vertebrates this corresponds to the posterior side of the developing retina (Baye & Link, 2008)
77 (Figure 1A). In the cephalopod, fixed time point data suggests that mitosis occurs on the anterior
78 side of the developing retina, inverted relative to vertebrates (Koenig et al., 2016) (Figure 1A).
79 These observations suggest that neurogenesis may be more similar to vertebrate processes than
80 previously observed in other invertebrates and lead us to ask whether cephalopod retinal
81 progenitor cells undergo interkinetic nuclear migration and how cells differentiate within this
82 epithelium.
83
84
85 **Results**
86 **Cell cycle in the developing squid retina**
87 Previous work in the squid retina showed that at Arnold stage 23, a three hour BrdU pulse
88 resulted in incorporation throughout the retina (Arnold, 1965; Koenig et al., 2016). This long pulse
89 provided time for cells to move after incorporation, making it difficult to determine if only a subset
90 of cells may be proliferative. To more precisely understand cell cycle state and organization in the
91 early retina, we performed a 10 minute BrdU pulse experiment, fixing immediately, and co-labeling
92 with phosphohistone H3 immunofluorescence (PH3) (Figure 1B). We see that BrdU incorporation
93 in S-phase cells is restricted to the posterior of the retina after 10 minutes. We also find PH3
94 positive labeled nuclei, in late G2 and M phase, on the anterior surface of the retina, supporting
95 previous observations. The lack of BrdU incorporation in the anterior retina suggests that some
96 cells are already post-mitotic.
97 If cells are undergoing interkinetic nuclear migration, we would expect BrdU positive nuclei
98 to eventually migrate apically to divide. To test this hypothesis, we chased our 10 minute BrdU
99 pulse, sampling embryos every ten minutes for 110 minutes, again co-labeling with PH3 (Figure
100 1C). We found that at 80 minutes after the pulse we see BrdU positive/PH3 positive cells in the

101 anterior retina, suggesting that nuclei are migrating apically to divide (Figure 1D). If proliferative
102 cells in the posterior retina eventually exit the cell cycle and join the cells in the anterior retina, we
103 would expect to find BrdU positive/PH3 negative cells in the anterior retina. Indeed, at 110 minutes
104 we find BrdU positive, PH3 negative cells in the anterior retina (Figure 1E). Together, these data
105 suggest that cells in the cell cycle have nuclei residing in the posterior retina and these nuclei
106 migrate apically to divide. Eventually these cells exit the cell cycle, and their cell bodies migrate
107 to the anterior of the retina. These data are consistent with cells undergoing interkinetic nuclear
108 migration, with post-mitotic cells segregated apically.
109
110 ***In vivo* observations of nuclear migration and proliferation in the squid retinal epithelium**
111 While fixed tissue experiments support our hypothesis, to fully understand the dynamics
112 of these cell behaviors, it is necessary to observe development *in vivo*. This required us to develop
113 a cell-resolution live-imaging protocol in cephalopods (Figure 2A). We injected fluorescent
114 Dextran to broadly label cell membranes and performed >9 hour developmental time course
115 imaging experiments of the squid retina at stage 23 (Figure 2A). Within these time course
116 datasets, we were able to track individual cells migrating from the basal lamina to the apical side
117 of the retina, where they mitose, and migrate basally again (Figure 2B, 2C, Movie S1, S2, S3).
118 These data confirm the process of interkinetic nuclear migration in the squid retina. From these
119 data we are able to calculate nuclear velocity and were able to assess that this migratory behavior
120 is similar in velocity to movement described in the vertebrate retina (Figure 2D) (Norden et al.,
121 2009).
122 The molecular motors contributing to nuclear migration have been interrogated in a
123 number of developmental contexts and some tissues rely exclusively or primarily on actomyosin,
124 while others require microtubules contribution to promote migration (Kosodo, 2012; E. J. Meyer
125 et al., 2011; Norden, 2017). To understand the contribution of these motors to nuclear migration
126 in the squid retina, we treated stage 23 embryos with either the actin polymerization inhibitor
127 cytochalasin D or the microtubule polymerization inhibitor nocodazole for seven hours and fixed
128 immediately. The impact of these inhibitors on nuclear migration was assessed using
129 immunofluorescence for PH3 (Figure 2E-2H). We find that nuclei positive for PH3 in the
130 cytochalasin D treated retinas are often displaced from the mitotic zone (MZ), defined as the
131 region of the epithelium containing nuclei abutting the most apical membrane. We find a small
132 percentage of PH3 positive nuclei in controls are also outside the mitotic zone, which are likely at
133 the end of G2, migrating toward the apical surface. Quantifying these differences, we see a
134 significant increase in cells outside the mitotic zone in our CytoD treated embryos suggesting

135 actin polymerization is required for nuclear migration. In addition, we see defects in migration in
136 nocodazole treated embryos; a population of PH3 positive nuclei accumulated at the apical
137 surface of the retina. This is what we would expect if microtubules were not required for migration,
138 as cells that have successfully migrated apically would then arrest and accumulate in M phase as
139 microtubules are required for mitosis. However, in addition to this accumulation, we find a
140 subpopulation of PH3 positive cells away from the mitotic zone, suggesting that microtubules play
141 a role in nuclear migration in the cephalopod retina.
142 In addition to nuclear movement, we were also able to assess the angle of cell division in
143 the epithelium. Symmetrical and asymmetrical cell division is an essential aspect of regulating
144 self-renewal, cell cycle exit and cell fate commitment during neurogenesis in multiple organisms
145 (Yu et al., 2006; Zigman et al., 2005); (Dehay & Kennedy, 2007). Overwhelmingly, we find most
146 mitoses observed to be symmetrical relative to the apical surface of the epithelium (Figure 2I,
147 Movie S2). We hypothesize that these divisions are self-renewing. We also observe
148 approximately 10% of cell divisions to be angled relative to the apical surface (Figure 2I, 2J & 2K,
149 Movie S3). We determined that symmetrical cell divisions had a division plane with an angle
150 relative to the apical surface between 60-90 degrees and asymmetrical divisions between 30-60
151 degrees (Figure 2K). We did not observe any cell divisions perpendicular to the apical surface,
152 (0-30 degrees) as have been observed in other systems (Knoblich, 2008; Morin & Bellaïche,
153 2011). We hypothesize that these asymmetric cell divisions may contribute to cells exiting the cell
154 cycle, however we were unable to follow cells long enough during live imaging to confirm this
155 hypothesis.
156
157 **Molecular identity during retinal neurogenesis**
158 To better understand the molecular state correlated with the cell cycle organization
159 observed in our BrdU and live imaging experiments, we sought to identify molecular markers that
160 help define differentiation trajectories in the cephalopod retina. We analyzed spatiotemporal
161 expression of thirteen candidate neurogenesis markers in the retina (Figure 3A, Supplemental
162 Figure 1, Supplemental Figure 2). We identified that in early retinal development, stage 21,
163 *DpSoxB1* is homogeneously expressed across the retinal epithelium. At stage 23 the retina is
164 divided across the apical-basal axis with *DpSoxB1* found on the basal side of the retina,
165 correlating with BrdU incorporation, and *DpEphR* is expressed on the apical side. At stage 25 we
166 see the maintenance of segregated *DpSoxB1* and *DpEphR* expression, as well as the first
167 evidence of the terminal differentiation markers *DpRetinochrome* and *DpRhodopsin*. At stage 27,
168 the first evidence of the basal membrane is apparent, which is correlated with a loss of strict

169 segregation of *DpSoxB1* and *DpEphR* expression. We hypothesize this change is a result of cell-
170 body migration or mixing, with apical cells moving to the posterior of the retina and basal cells
171 moving to the anterior of the retina. We hypothesize that this resorting moves the post-mitotic
172 cells to the posterior where they will become the first photoreceptor cell bodies to migrate behind
173 the basal membrane. This is supported by previous observations of nuclei crossing the basal
174 membrane (Koenig et al., 2016). Supporting this hypothesis, we find that *DpSoxB1* expression
175 is never found posterior to the basal membrane. However, *DpEphR* is found on both sides of the
176 membrane until hatching. At hatching *DpEphR* is isolated to a subset of cells posterior to the basal
177 membrane. These cells may be maturing photoreceptor cells that have recently migrated to the
178 photoreceptor cell layer during hatching and post-hatching stage growth. Terminal differentiation
179 markers span both sides of the basal membrane at hatching. We hypothesize that *DpRhodopsin*
180 is expressed exclusively in the photoreceptor cells and is being trafficked to the outer segment
181 and that *DpRetinochrome* is expressed in both the photoreceptor cells and support cells.
182 This candidate gene survey suggests cell differentiation trajectories in the retina (Figure
183 3B, 3C). Our photoreceptor cell differentiation trajectory starts as *DpSoxB1* positive retinal
184 progenitor cells undergoing interkinetic nuclear migration in the pseudostratified epithelium.
185 These cells transition to *DpEphR* positive cells and become post-mitotic. We hypothesize that this
186 is the result of an asymmetric cell division. Eventually *DpEphR* expressing cells mature and begin
187 to express terminal differentiation markers, ultimately completing differentiation when they
188 exclusively express *DpRhodopsin* and *DpRetinochrome.*
189 We hypothesize a simple differentiation trajectory for the proliferative support cell
190 population (Figure 3B & 3C). These cells start as *DpSoxB1* positive retinal progenitor cells,
191 undergoing interkinetic nuclear migration. This self-renewing population is maintained throughout
192 development. During cell mixing at stage 27, *DpSoxB1* positive support cells begin to express
193 *DpRetinochrome,* migrate anterior in the retina and remain in the cell cycle. The
194 *DpSoxB1/DpRetinochrome* expressing support cells may be a long term stem cell population in
195 the retina.
196
197 **Notch regulates retinal progenitor identity in the cephalopod**
198 Our data show that BrdU incorporation correlates with *DpSoxB1* expression and *DpEphR*
199 expression correlates with post mitotic cells. Our BrdU chase experiments suggest that *DpSoxB1*
200 cells likely become *DpEphR* cells over time (Figure 4A, 4B & 4C). Notch signaling is a well-known
201 regulator of cell cycle exit and differentiation. Previous work showed that inhibiting Notch signaling
202 in the cephalopod using the gamma-secretase inhibitor DAPT led to a loss of BrdU incorporation

203 in the retina, showing that Notch was inhibiting cell cycle exit. We were interested in understanding
204 the role of Notch signaling in regulating cell fate trajectories in conjunction with proliferation. We
205 first performed *in situ* hybridization for Notch signaling pathway members in the retina (Figure 4D
206 and Supplemental Figure 3). If Notch signaling is important for maintaining progenitor fate, we
207 would expect Notch and Hes to be enriched in retinal progenitor cells. We find that *DpNotch* and
208 *DpHes-1* expression is correlated with *DpSoxB1* expression and retinal progenitor identity (Figure
209 4D and Supplemental Figure 3). Interestingly, we find that Delta is ubiquitously expressed during
210 these stages (Supplemental Figure 3). We also find *DpNotch* expressed in a limited number of
211 nuclei on the apical side of the retina. We wanted to know if this expression correlated with nuclei
212 that had migrated apically to divide. We performed *in situ* hybridization for *DpNotch* in conjunction
213 with PH3 immunofluorescence and found that apical *DpNotch* expression is correlated with PH3
214 positive nuclei (Figure 4E). Inheritance of Notch mRNA may be an important part of maintaining
215 progenitor cell identity.
216 To assess the role of Notch in cell fate we used the gamma secretase inhibitor DAPT to
217 inhibit active signaling. Embryos were treated with DAPT or DMSO starting at stage 23 for 24
218 hours. Eyes were dissected and pooled. RNA was extracted from three experimental and control
219 samples and sequenced. 2242 genes were differentially expressed between DAPT and control
220 eyes with a p-value of less than 0.05 (Supplemental Table 1). *DpSoxB1* was found downregulated
221 and *DpEphR* was found upregulated in the dataset, but these changes were not deemed
222 statistically significant. DAPT compared to control eye samples showed both up and down
223 regulation in neural and sensory markers. Of note is the down regulation of Rhodopsin and other
224 G-protein coupled receptor related genes (Figure 4F). In addition, cell cycle related genes were
225 downregulated, which is expected as DAPT treatment leads to cell cycle exit in the squid retina
226 (Koenig et al., 2016) (Figure 4G). Finally, DAPT versus control eyes showed significant changes
227 in cell signaling genes, suggesting that Notch may self-regulate as well as interact with other
228 signaling pathways in the retina, including VEGFR, BMP and Wnt (Figure 4H).
229 To confirm changes in gene expression identified in the RNA-seq analysis, we performed
230 *in situ* hybridization studies on control and DAPT embryos (Figure 4I and Supplemental Figure 4
231 and Supplemental Figure 5). We confirm trends shown in the RNA-seq results. Specifically, we
232 find a loss of *DpNotch* expression, a downregulation of *DpRhodopsin,* and a complete loss of
233 *DpSoxB1* in DAPT treated retinas (Figure 4I). We also observe a gain of expression of *DpEphR*
234 and synaptic transmission related gene, *DpSec-1,* in the posterior retina (Figure 4I). Interestingly,
235 we see ectopic expression of *DpVEGFR* in a subpopulation of cells in the DAPT treated retinas
236 relative to control. The unusual placement of ectopic expression of *DpVEGFR* may be

compounded by the disorganization of the DAPT treated retinas. The complete loss of *DpSoxB1* and the ectopic expression of *DpEphR* shows that DAPT inhibition not only results in changes in cell cycle state, but also changes molecular fate in the squid retina. These data suggest that Notch signaling is required to maintain retinal progenitor identity in the squid.

Discussion

In the current study we have characterized the nuclear oscillatory behaviors of retinal progenitor cells in squid. We have defined the molecular markers for progenitor, post-mitotic, and fully differentiated cells in the retina and we have shown that Notch signaling is regulating both cell cycle and molecular identity during retinal development. The importance of these findings is in comparison to what is known about neurogenesis in other systems.

Pseudostratified epithelia and interkinetic nuclear migration have been observed in multiple tissue types and across multiple species (E. J. Meyer et al., 2011). In the nervous system, pseudostratification was historically considered a vertebrate specific developmental trait, which was responsible for the large size of the central nervous system. Elaborate tissue-level morphogenesis is has not been observed in invertebrate neural development, where individual cells delaminate or ingress from a simple or stratified neuroepithelium, sometimes divide, and then migrate to their final destination to differentiate (N. P. Meyer & Seaver, 2009; Sur et al., 2020); (Byrne, 2019; Hartenstein & Stollewerk, 2015). However, interkinetic nuclear migration has been described in the *Drosophila* optic lobe (Egger et al., 2007). In this case, the apicobasal distance of migration is significantly smaller than vertebrate neurogenic tissues and cells delaminate from the edge of the proliferative epithelium and migrate to their final destination to differentiate (Egger et al., 2007; Holguera & Desplan, 2018; Strzyz et al., 2016). This process has been compared to “conveyor belt” neurogenesis found in the zebrafish ciliary and tectal marginal zones, where, during long term growth, cells are progressively added from the edge of a pseudostratified stem cell population (Joly et al., 2016). The behavior described in the squid retina is unusual because of its unique similarity to early neurogenesis in vertebrate species, which is characterized by waves of differentiation within the pseudostratified epithelium (Agathocleous & Harris, 2009; Livesey & Cepko, 2001). In the squid, we show that apicobasal height of the epithelium is similar to vertebrate tissues, cells undergo interkinetic nuclear migration while proliferative, and cells remain within the bounds of the epithelium after delaminating and differentiating. The functional difference between conveyor belt neurogenesis versus within-epithelium differentiation is unclear, but the architecture of the epithelium may provide physical landmarks or signaling information important for proper organization.

271 Although pseudostratified neurogenesis is found in the cephalopod retina, the cell biology
272 of chordal or central nervous system neurogenesis is still not well described. It has been reported
273 that cells migrate from the lateral lip tissue, an embryonic neurogenic tissue found in the
274 cephalopod embryo to regions within the brain but pseudostratification of the lateral lips is not
275 apparent (Deryckere et al., 2021). Cephalopod central nervous system development may more
276 closely resemble neurogenesis found in other invertebrates or molluscs (Deryckere et al., 2021;
277 Marthy, 1987). With a central nervous system composed of significantly more cells than other
278 Spiralians and requiring long distance cell migration, it is likely that cephalopods have evolved
279 lineage specific mechanisms to manage this process.
280 Interestingly, in the squid, candidate gene expression of neurogenic factors also differs
281 significantly between the developing retina and other brain regions. This includes a lack of
282 expression of the canonical neurogenic ELAV, *DpELAV*, in the retina, an RNA binding protein
283 commonly found in differentiating neurons across species (Akamatsu et al., 2005; Denes et al.,
284 2007; N. P. Meyer & Seaver, 2009; Nakanishi et al., 2012; Nomaksteinsky et al., 2009). bHLH
285 factors *DpNeuroD* and *DpNeuroG*, both with orthologs that have roles in neural specification and
286 differentiation in many animals, are expressed in the lateral lips and brain in *D. pealeii* and other
287 cephalopods but are completely absent for the retina (Supplemental Figure 2) (Buresi et al.,
288 2013; Deryckere et al., 2021; Shigeno et al., 2015). However, it has been reported in *Octopus*
289 *vulgaris* that achaete-scute homolog *Ov-ascl1*, a third proneural bHLH transcription factor, is
290 expressed in the retina (Deryckere et al., 2021). Furthermore, SoxB1, required to maintain neural
291 precursors cells in vertebrates (Sox1, 2 and 3) and neuroblasts in *Drosophila* (SoxNeuro and
292 Dichaete), is also a retinal progenitor marker in cephalopods (Buescher et al., 2002; Bylund et al.,
293 2003; Ferrero et al., 2014; Holmberg et al., 2008; Overton et al., 2002; Taranova et al., 2006). We
294 also find that both cephalopod-specific *DpELAVL* paralogs show expression that suggests a role
295 in neurogenesis in both the retina and brain (Supplemental Figure 2).
296 Finally, we show that Notch signaling is maintaining molecular identity of the progenitor
297 population in the squid retina, and that the loss of Notch signaling leads to expression of the post-
298 mitotic marker *DpEphR*. In the vertebrate retina, the premature loss of Notch signaling leads to
299 the differentiation of early born cell types (Perron & Harris, 2000). In *D. pealeii*, we see a decrease
300 in *DpRhodopsin* expression, suggesting cells may have arrested in this immature post-mitotic
301 state. We also see the maintenance in *DpRetinochrome* expression, which may be evidence of
302 differing trajectories of these cell types during neurogenesis.
303 The function of pseudostratification and interkinetic nuclear migration during development
304 remains unclear, however our data sheds new light on old hypotheses. In particular,

305 pseudostratification may aid in intracellular organization, as we see significant mRNA localization
306 in our data, including mRNA transport correlated with nuclear migration. It may also be that the
307 physics and dynamics of pseudostratified epithelia are better at accommodating increased
308 proliferation or provides an organizational scaffold for the differentiating network of neurons. It will
309 be interesting to apply new fluid dynamics approaches used to study vertebrate neurogenesis to
310 the cell biology of this similar tissue (Azizi et al., 2020). Ultimately, the evidence we have
311 generated in cephalopods suggests that vertebrate-like cell behaviors during neurogenesis are
312 not exclusive to the chordate lineage. With greater sampling we may better understand the
313 evolutionary changes that contribute to the diversity and complexity we see.
314
315
316 **Methods**
317 **Animal Husbandry**
318 *Doryteuthis pealeii* egg sacks were obtained from the Marine Biological Labs. Egg sacks were
319 kept at 20 degrees Celsius in 20 gallon aquaria in artificial seawater under a day/night cycle.
320 Although not required, European guidelines for cephalopod research were followed.
321
322 **Cloning and *in situ* Hybridization**
323 Primers were designed using Primer3 in the Geneious software package version 2020.04
324 (https://www.geneious.com) and primer sequences are reported in Supplemental Table 2. Genes
325 were cloned into pGEM-T Easy vector and confirmed with Sanger sequencing and DIG-labeled
326 RNA probes were synthesized as previously reported (Koenig et al., 2016). Embryos were fixed
327 overnight at 4 degrees Celsius, washed and dehydrated stepwise into 100% ethanol. Embryos
328 were embedded, paraffin sectioned and *in situ* hybridization was performed as previously reported
329 (Neal et al., n.d.). All *in situs* were replicated in at least three embryos, across multiple separate
330 *in situ* experiments. Slides were stained overnight with Sytox-Green 1:1000 overnight, mounted
331 using ImmunoHistoMount (Abcam) and imaged on a Zeiss Axioskop 2.
332
333 **BrdU Experiments**
334 Embryos were bathed in BrdU (10 mM) in pen-strep seawater for 10 minutes as previously
335 described (Koenig et al., 2016). Embryos were fixed immediately, and the remaining embryos
336 were moved into pen-strep seawater. Groups of 10-15 embryos were fixed every ten minutes for
337 two hours. Embryos were fixed overnight at 4 degrees and washed out into PBS-Tween. Embryos
338 were stepped into 30% sucrose and embedded in tissue freezing medium and sectioned as
339 previously described (Koenig et al., 2016). Antigen-retrieval and immunofluorescence was
340 performed as previously described. BrdU antibody (Abcam ab6326) at concentration 1:250.
341 Phosphohistone H3 antibody (Sigma-Aldrich 06-570) was used at concentration 1:300.
342 Secondary antibodies goat anti-rat Alexa Fluor 488 and goat anti rabbit Alexa Fluor 647
343 (Invitrogen). Sections were counterstained with SYTOX-Green at 1:1000. Sections were imaged
344 on a Zeiss LSM 880 or Zeiss LSM 980.
345

346 **Live-imaging experiments**
347 Embryos were dissected from egg cases. The vitreous space was injected using a pico-liter
348 microinjector with Dextran Alexa Fluor 488 10,000 MW (D22910) at stage 23. Embryos were
349 embedded in 1% low melt agarose in seawater and mounted in cover glass bottom dishes
350 (100503-366). Embryos were immersed in pen strep seawater. Embryos were imaged on a Zeiss
351 880. Embryos were imaged every ten minutes for at least nine hours.
352
353 **Imaging analysis**
354 Image analysis was performed in Fiji (Schindelin et al., 2012). Intensity range was adjusted in Fiji
355 to better identify cell membranes. Drift correction was performed using Fiji plugin CoordinateShift
356 (written by Housei Wada, https://signaling.riken.jp/en/en-tools/imagej/). Nuclear tracking was
357 performed both manually and using Fiji plugin Trackmate (Robertson, 2018; Schindelin et al.,
358 2012). Tracks were visualized and distance and velocity measurements were obtained from
359 Trackmate and plotted graphically, normalizing to the highest point in migration.
360
361 ***Ex ovo* and Drug Treatments**
362 Embryos were treated in 20uM DAPT solution or DMSO control in filter-sterilized, Pen-Strep
363 seawater starting at stage 23 for 24 hours and fixed immediately as previously described (Koenig
364 et. al, 2016). Embryos were bathed in 5uM Nocodazole (M1404-2MG, Sigma-Aldrich) and 5uM
365 Cytochalasin D (C8273-1MG, Sigma-Aldrich) for 7 hours and fixed immediately.
366
367 **RNA-seq and Bioinformatics**
368 Stage 23 embryos were treated with the gamma-secretase inhibitor DAPT at 20um in filter
369 sterilized sea water for 24 hours and Control embryos were treated with the equivalent amount of
370 DMSO, as previously described (Koenig et al., 2016). DAPT and Control eyes were dissected,
371 pooled and macerated in TRIzol and stored at -80 degrees Celsius. RNA was extracted using a
372 standard TRIzol (Invitrogen #15596026) chloroform extraction and passed through a gDNA
373 eliminator mini-spin column (Qiagen #1030958). RNA was precipitated with isopropanol and then
374 again precipitated with ethanol and checked for quality. Library prep and sequencing was
375 performed at the Bauer Core at Harvard University. RNA-seq libraries were generated using the
376 Kapa mRNA-Hyper Prep kit with Poly-A Selection (Roche, Basal) and were sequenced on the
377 Illumina NovaSeq (>70 million 2x150 bp sequences) (Illumina, San Diego, CA).
378 Sequence quality control was performed according to the best practice recommendation
379 on the Harvard FAS Informatics pipeline (https://informatics.fas.harvard.edu/best-practices -for-
380 de-novo-transcriptome-assembly-with-trinity.html). Erroneous kmers were removed from the
381 paired end Illumina dataset using rCorrector. Reads with Ns or other low complexity pairs were
382 removed using a custom python script provided by the Harvard Informatics GitHub
383 (FilterUncorrectabledPEfastq.py). Adapters and low quality bases were removed using
384 TrimGalore! Reads that mapped using Bowtie2 to the rRNA databases SILVA 132 SSURef Nr99
385 tax and SILVA 132 LSUParc tax were removed. Pseudomapping was performed by Kallisto with
386 100 bootstraps to a previously published whole embryo transcriptome (Koenig et al., 2016).
387 Transcript abundances were imported using tximport (https://bioconductor.org/packages/3.7/ b
388 ioc/vignettes/tximport/inst/doc/tximport.html#use-with-downstream-bioconductor-dge-packages)
389 into DESeq2 using the Kallisto abundance.h5 files. Differential gene expression was determined

by importing transcript level abundances and gene level offset using *DESeqDataSetFromTximport* (Soneson et al., 2015). The DESeq2 pipeline was run and differentially expressed genes were considered with a p value of .05 and log2 fold change of above 1 and below -1. All genes shown in the chord plots in figure 4 meet these criteria with the exception of Notch which was included with a log2 fold change of -0.83. GO annotations were identified using the DAVID functional annotation tool (Huang et al., 2007). Chord plots were generated using the R package GOPlot (Walter et al., 2015) and gplots (*Website*, n.d.)Warnes(*Website*, n.d.).

Funding

This work was supported by a grant from the Office of the NIH Director 1DP5OD023111-01 and the John Harvard Distinguished Science Fellowship awarded to K.M.K.

Acknowledgements

We would like to thank the Srivastava lab for helpful discussions and Mansi Srivastava and Jeffrey Gross for comments on the manuscript. We thank Kevin Woods and the John Harvard Distinguished Science Fellows community for support and the Marine Biological Labs and the Marine Resources Center for assistance and access to embryos.

Author Contributions

K.M.K conceived of the study with input from F.N., C.M.D. and S.N.; K.M.K, F.N., C.M.D., S.N., A.Z., and A.L. performed experiments. K.J.M. performed phylogenetic analyses. K.M.K., C.M.D and K.J.M. wrote the manuscript in consultation with all authors.

References

Agathocleous, M., & Harris, W. A. (2009). From Progenitors to Differentiated Cells in the Vertebrate Retina. In *Annual Review of Cell and Developmental Biology* (Vol. 25, Issue 1, pp. 45–69). https://doi.org/10.1146/annurev.cellbio.042308.113259

Akamatsu, W., Fujihara, H., Mitsuhashi, T., Yano, M., Shibata, S., Hayakawa, Y., Okano, H. J., Sakakibara, S.-I., Takano, H., Takano, T., Takahashi, T., Noda, T., & Okano, H. (2005). The RNA-binding protein HuD regulates neuronal cell identity and maturation. *Proceedings of the National Academy of Sciences of the United States of America*, *102*(12), 4625–4630. https://doi.org/10.1073/pnas.0407523102

Arnold, J. M. (1965). NORMAL EMBRYONIC STAGES OF THE SQUID, LOLIGO PEALII (LESUEUR). In *The Biological Bulletin* (Vol. 128, Issue 1, pp. 24–32). https://doi.org/10.2307/1539386

Azizi, A., Herrmann, A., Wan, Y., Buse, S. J., Keller, P. J., Goldstein, R. E., & Harris, W. A. (2020). Nuclear crowding and nonlinear diffusion during interkinetic nuclear migration in the zebrafish retina. *eLife*, *9*. https://doi.org/10.7554/eLife.58635

Baye, L. M., & Link, B. A. (2008). Nuclear migration during retinal development. In *Brain Research* (Vol. 1192, pp. 29–36). https://doi.org/10.1016/j.brainres.2007.05.021

Bertrand, V., & Hobert, O. (2010). Lineage programming: navigating through transient regulatory states via binary decisions. *Current Opinion in Genetics & Development*, *20*(4), 362–368. https://doi.org/10.1016/j.gde.2010.04.010

Buescher, M., Hing, F. S., & Chia, W. (2002). Formation of neuroblasts in the embryonic central nervous system of Drosophila melanogaster is controlled by SoxNeuro. *Development* , *129*(18), 4193–4203. https://www.ncbi.nlm.nih.gov/pubmed/12183372

Buresi, A., Canali, E., Bonnaud, L., & Baratte, S. (2013). Delayed and asynchronous ganglionic maturation during cephalopod neurogenesis as evidenced by Sof-elav1 expression in embryos of Sepia officinalis (Mollusca, Cephalopoda). *The Journal of Comparative*

Neurology, *521*(7), 1482–1496. https://doi.org/10.1002/cne.23231

Bylund, M., Andersson, E., Novitch, B. G., & Muhr, J. (2003). Vertebrate neurogenesis is counteracted by Sox1–3 activity. In *Nature Neuroscience* (Vol. 6, Issue 11, pp. 1162–1168). https://doi.org/10.1038/nn1131

Byrne, J. H. (2019). *The Oxford Handbook of Invertebrate Neurobiology*. Oxford University Press. https://play.google.com/store/books/details?id=O_iEDwAAQBAJ

Dehay, C., & Kennedy, H. (2007). Cell-cycle control and cortical development. In *Nature Reviews Neuroscience* (Vol. 8, Issue 6, pp. 438–450). https://doi.org/10.1038/nrn2097

Denes, A. S., Jékely, G., Steinmetz, P. R. H., Raible, F., Snyman, H., Prud'homme, B., Ferrier, D. E. K., Balavoine, G., & Arendt, D. (2007). Molecular architecture of annelid nerve cord supports common origin of nervous system centralization in bilateria. *Cell*, *129*(2), 277–288. https://doi.org/10.1016/j.cell.2007.02.040

Deryckere, A., Styfhals, R., Elagoz, A. M., Maes, G. E., & Seuntjens, E. (2021). Identification of neural progenitor cells and their progeny reveals long distance migration in the developing octopus brain. *eLife*, *10*. https://doi.org/10.7554/eLife.69161

Egger, B., Boone, J. Q., Stevens, N. R., Brand, A. H., & Doe, C. Q. (2007). Regulation of spindle orientation and neural stem cell fate in the Drosophila optic lobe. *Neural Development*, *2*, 1. https://doi.org/10.1186/1749-8104-2-1

Ferrero, E., Fischer, B., & Russell, S. (2014). SoxNeuro orchestrates central nervous system specification and differentiation in Drosophila and is only partially redundant with Dichaete. *Genome Biology*, *15*(5), R74. https://doi.org/10.1186/gb-2014-15-5-r74

Gagnon, Y. L., Sutton, T. T., & Johnsen, S. (2013). Visual acuity in pelagic fishes and mollusks. *Vision Research*, *92*, 1–9. https://doi.org/10.1016/j.visres.2013.08.007

Hartenstein, V., & Stollewerk, A. (2015). The evolution of early neurogenesis. *Developmental Cell*, *32*(4), 390–407. https://doi.org/10.1016/j.devcel.2015.02.004

Holguera, I., & Desplan, C. (2018). Neuronal specification in space and time. *Science*,

362(6411), 176–180. https://doi.org/10.1126/science.aas9435

Holmberg, J., Hansson, E., Malewicz, M., Sandberg, M., Perlmann, T., Lendahl, U., & Muhr, J. (2008). SoxB1 transcription factors and Notch signaling use distinct mechanisms to regulate proneural gene function and neural progenitor differentiation. *Development* , *135*(10), 1843–1851. https://doi.org/10.1242/dev.020180

Huang, D. W., Sherman, B. T., Tan, Q., Kir, J., Liu, D., Bryant, D., Guo, Y., Stephens, R., Baseler, M. W., Clifford Lane, H., & Lempicki, R. A. (2007). DAVID Bioinformatics Resources: expanded annotation database and novel algorithms to better extract biology from large gene lists. In *Nucleic Acids Research* (Vol. 35, Issue suppl_2, pp. W169–W175). https://doi.org/10.1093/nar/gkm415

Joly, J.-S., Recher, G., Brombin, A., Ngo, K., & Hartenstein, V. (2016). A Conserved Developmental Mechanism Builds Complex Visual Systems in Insects and Vertebrates. *Current Biology: CB*, *26*(20), R1001–R1009. https://doi.org/10.1016/j.cub.2016.08.017

Knoblich, J. A. (2008). Mechanisms of asymmetric stem cell division. *Cell*, *132*(4), 583–597. https://doi.org/10.1016/j.cell.2008.02.007

Koenig, K. M., & Gross, J. M. (2020). Evolution and development of complex eyes: a celebration of diversity. *Development* , *147*(19). https://doi.org/10.1242/dev.182923

Koenig, K. M., Sun, P., Meyer, E., & Gross, J. M. (2016). Eye development and photoreceptor differentiation in the cephalopod Doryteuthis pealeii. *Development* , *143*(17), 3168–3181. https://doi.org/10.1242/dev.134254

Kosodo, Y. (2012). Interkinetic nuclear migration: beyond a hallmark of neurogenesis. *Cellular and Molecular Life Sciences: CMLS*, *69*(16), 2727–2738. https://doi.org/10.1007/s00018-012-0952-2

Livesey, F. J., & Cepko, C. L. (2001). Vertebrate neural cell-fate determination: lessons from the retina. *Nature Reviews. Neuroscience*, *2*(2), 109–118. https://doi.org/10.1038/35053522

Marthy, H.-J. (1987). Ontogenesis of the Nervous System in Cephalopods. In *Nervous Systems*

in Invertebrates (pp. 443–459). https://doi.org/10.1007/978-1-4613-1955-9_15

Meyer, E. J., Ikmi, A., & Gibson, M. C. (2011). Interkinetic Nuclear Migration Is a Broadly Conserved Feature of Cell Division in Pseudostratified Epithelia. In *Current Biology* (Vol. 21, Issue 6, pp. 485–491). https://doi.org/10.1016/j.cub.2011.02.002

Meyer, N. P., & Seaver, E. C. (2009). Neurogenesis in an annelid: Characterization of brain neural precursors in the polychaete Capitella sp. I. In *Developmental Biology* (Vol. 335, Issue 1, pp. 237–252). https://doi.org/10.1016/j.ydbio.2009.06.017

Morin, X., & Bellaïche, Y. (2011). Mitotic spindle orientation in asymmetric and symmetric cell divisions during animal development. *Developmental Cell*, *21*(1), 102–119. https://doi.org/10.1016/j.devcel.2011.06.012

Nakanishi, N., Renfer, E., Technau, U., & Rentzsch, F. (2012). Nervous systems of the sea anemone Nematostella vectensis are generated by ectoderm and endoderm and shaped by distinct mechanisms. *Development* , *139*(2), 347–357. https://doi.org/10.1242/dev.071902

Neal, S., McCulloch, K. J., Napoli, F., Daly, C. M., Coleman, J. H., & Koenig, K. M. (n.d.). *Co-option of the Limb Patterning Program in Cephalopod Lens Development*. https://doi.org/10.1101/2021.04.22.441006

Nomaksteinsky, M., Röttinger, E., Dufour, H. D., Chettouh, Z., Lowe, C. J., Martindale, M. Q., & Brunet, J.-F. (2009). Centralization of the deuterostome nervous system predates chordates. *Current Biology: CB*, *19*(15), 1264–1269. https://doi.org/10.1016/j.cub.2009.05.063

Norden, C. (2017). Pseudostratified epithelia – cell biology, diversity and roles in organ formation at a glance. In *Journal of Cell Science*. https://doi.org/10.1242/jcs.192997

Norden, C., Young, S., Link, B. A., & Harris, W. A. (2009). Actomyosin is the main driver of interkinetic nuclear migration in the retina. *Cell*, *138*(6), 1195–1208. https://doi.org/10.1016/j.cell.2009.06.032

Overton, P. M., Meadows, L. A., Urban, J., & Russell, S. (2002). Evidence for differential and redundant function of the Sox genes Dichaete and SoxN during CNS development in Drosophila. *Development* , *129*(18), 4219–4228. https://www.ncbi.nlm.nih.gov/pubmed/12183374

Packard, A. (1972). CEPHALOPODS AND FISH: THE LIMITS OF CONVERGENCE. In *Biological Reviews* (Vol. 47, Issue 2, pp. 241–307). https://doi.org/10.1111/j.1469-185x.1972.tb00975.x

Perron, M., & Harris, W. A. (2000). Determination of vertebrate retinal progenitor cell fate by the Notch pathway and basic helix-loop-helix transcription factors. *Cellular and Molecular Life Sciences: CMLS*, *57*(2), 215–223. https://doi.org/10.1007/PL00000685

Robertson, R. (2018). *Open and Extensible Control & Analytics Platform for Synchrophasor Data*. https://doi.org/10.2172/1468940

Schindelin, J., Arganda-Carreras, I., Frise, E., Kaynig, V., Longair, M., Pietzsch, T., Preibisch, S., Rueden, C., Saalfeld, S., Schmid, B., Tinevez, J.-Y., White, D. J., Hartenstein, V., Eliceiri, K., Tomancak, P., & Cardona, A. (2012). Fiji: an open-source platform for biological-image analysis. *Nature Methods*, *9*(7), 676–682. https://doi.org/10.1038/nmeth.2019

Shigeno, S., Parnaik, R., Albertin, C. B., & Ragsdale, C. W. (2015). Evidence for a cordal, not ganglionic, pattern of cephalopod brain neurogenesis. In *Zoological Letters* (Vol. 1, Issue 1). https://doi.org/10.1186/s40851-015-0026-z

Soneson, C., Love, M. I., & Robinson, M. D. (2015). Differential analyses for RNA-seq: transcript-level estimates improve gene-level inferences. *F1000Research*, *4*, 1521. https://doi.org/10.12688/f1000research.7563.2

Strzyz, P. J., Matejcic, M., & Norden, C. (2016). Heterogeneity, Cell Biology and Tissue Mechanics of Pseudostratified Epithelia: Coordination of Cell Divisions and Growth in Tightly Packed Tissues. *International Review of Cell and Molecular Biology*, *325*, 89–118.

https://doi.org/10.1016/bs.ircmb.2016.02.004

Sur, A., Renfro, A., Bergmann, P. J., & Meyer, N. P. (2020). Investigating cellular and molecular mechanisms of neurogenesis in Capitella teleta sheds light on the ancestor of Annelida. *BMC Evolutionary Biology*, *20*(1), 84. https://doi.org/10.1186/s12862-020-01636-1

Taranova, O. V., Magness, S. T., Fagan, B. M., Wu, Y., Surzenko, N., Hutton, S. R., & Pevny, L. H. (2006). SOX2 is a dose-dependent regulator of retinal neural progenitor competence. *Genes & Development*, *20*(9), 1187–1202. https://doi.org/10.1101/gad.1407906

Taverna, E., Götz, M., & Huttner, W. B. (2014). The cell biology of neurogenesis: toward an understanding of the development and evolution of the neocortex. *Annual Review of Cell and Developmental Biology*, *30*, 465–502. https://doi.org/10.1146/annurev-cellbio-101011-155801

Walter, W., Sánchez-Cabo, F., & Ricote, M. (2015). GOplot: an R package for visually combining expression data with functional analysis: Fig. 1. In *Bioinformatics* (Vol. 31, Issue 17, pp. 2912–2914). https://doi.org/10.1093/bioinformatics/btv300

Website. (n.d.). Gregory R. Warnes, Ben Bolker, Lodewijk Bonebakker, Robert Gentleman, Wolfgang Huber, Andy Liaw, Thomas Lumley, Martin Maechler, Arni Magnusson, Steffen Moeller, Marc Schwartz and Bill Venables (2015). gplots: Various R Programming Tools for Plotting Data. R package version 2.17.0. http://CRAN.R-project.org/package=gplots

Yamamoto, T., Tasaki, K., Sugawara, Y., & Tonosaki, A. (1965). FINE STRUCTURE OF THE OCTOPUS RETINA. *The Journal of Cell Biology*, *25*, 345–359. https://www.ncbi.nlm.nih.gov/pubmed/14287185

Young, J. Z. (1974). The central nervous system of Loligo. I. The optic lobe. *Philosophical Transactions of the Royal Society of London. Series B, Biological Sciences*, *267*(885), 263–302. https://doi.org/10.1098/rstb.1974.0002

Yu, F., Kuo, C. T., & Jan, Y. N. (2006). Drosophila Neuroblast Asymmetric Cell Division: Recent Advances and Implications for Stem Cell Biology. In *Neuron* (Vol. 51, Issue 1, pp. 13–20).

https://doi.org/10.1016/j.neuron.2006.06.016

Zechner, C., Nerli, E., & Norden, C. (2020). Stochasticity and determinism in cell fate decisions. *Development* , *147*(14). https://doi.org/10.1242/dev.181495

Zigman, M., Cayouette, M., Charalambous, C., Schleiffer, A., Hoeller, O., Dunican, D., McCudden, C. R., Firnberg, N., Barres, B. A., Siderovski, D. P., & Knoblich, J. A. (2005). Mammalian inscuteable regulates spindle orientation and cell fate in the developing retina. *Neuron*, *48*(4), 539–545. https://doi.org/10.1016/j.neuron.2005.09.030

Gregory R. Warnes, Ben Bolker, Lodewijk Bonebakker, Robert Gentleman, Wolfgang Huber, Andy Liaw, Thomas Lumley, Martin Maechler, Arni Magnusson, Steffen Moeller, Marc Schwartz and Bill Venables (2015). gplots: Various R Programming Tools for Plotting Data. R package version 2.17.0. http://CRAN.R-project.org/package=gplots

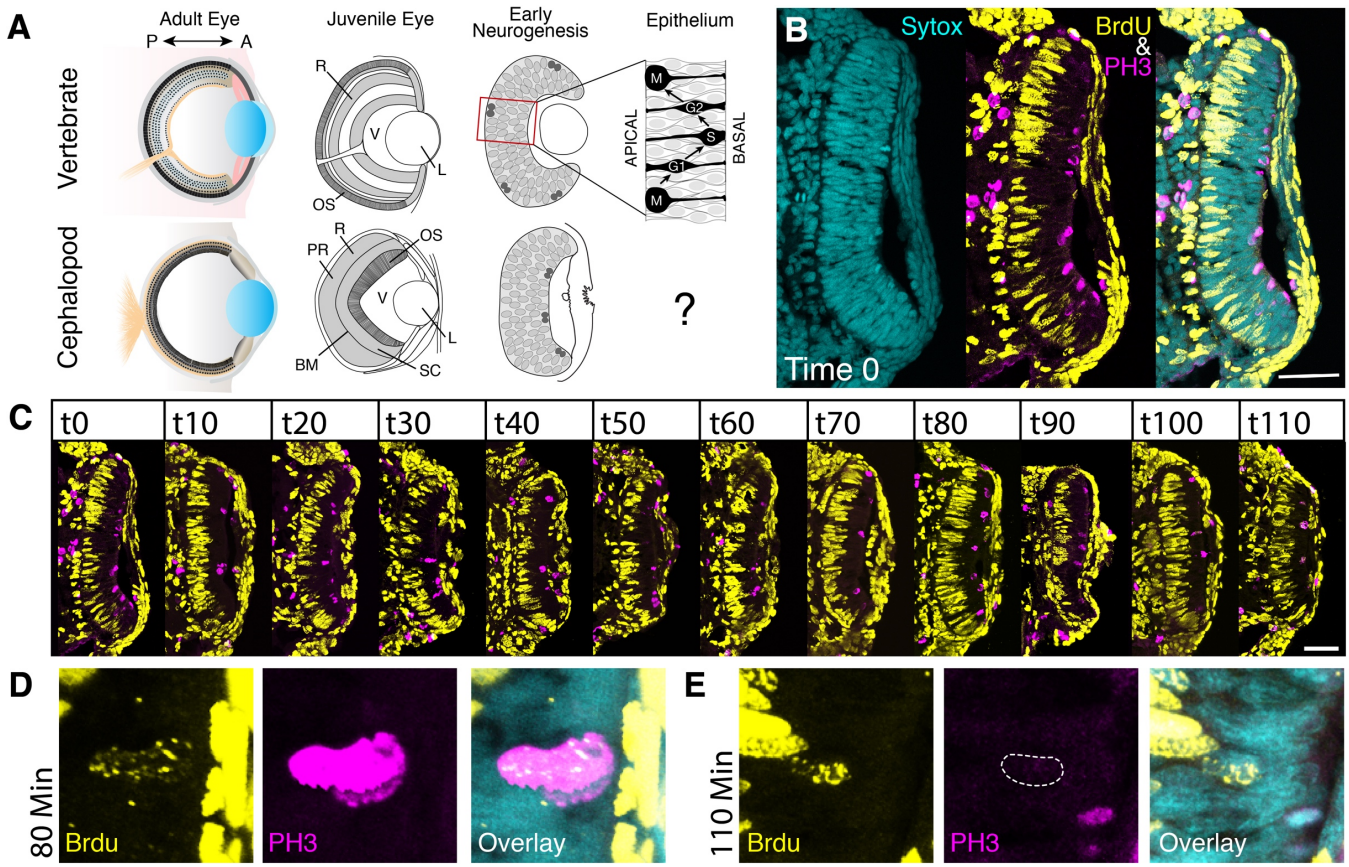

Figure 1: Cell cycle and nuclear migration in the squid retina assessed in fixed tissue. A. Schematic of the vertebrate and cephalopod eye at adult, juvenile and early stage development. Box shows enlargement of the vertebrate pseudostratified epithelium, apical to the left. Grey ovals are the nuclei distributed across the tissue early in development, darker grey nuclei are undergoing mitosis. *R:* Retina; *L:* Lens; *OS:* Outer Segment; *V:* Vitreous Space; PR: Photoreceptor Nuclear Layer; *SC:* Support Cell Layer; *BM:* Basal Membrane. **B.** 10 minute BrdU pulse and immediate fix (Time 0) BrdU/PH3 antibody stain shows BrdU incorporation on the posterior side of the epithelium (S-phase) and PH3 stain on the anterior side of the epithelium (M-phase). Scale 50um. **C.** BrdU/PH3 time course. 10 minute BrdU pulse, fixed every 10 minutes followed by BrdU/PH3 antibody stains. Scale 50um. Cell mixing is not observed until 80 minutes after pulse. **D.** 80 minutes after BrdU pulse is the first time point where BrdU+/PH3+ nuclei are found on the apical side of the retina. **E.** 110 minutes after pulse is the first time point where BrdU+/PH3- nuclei are found on the apical side of the retina.

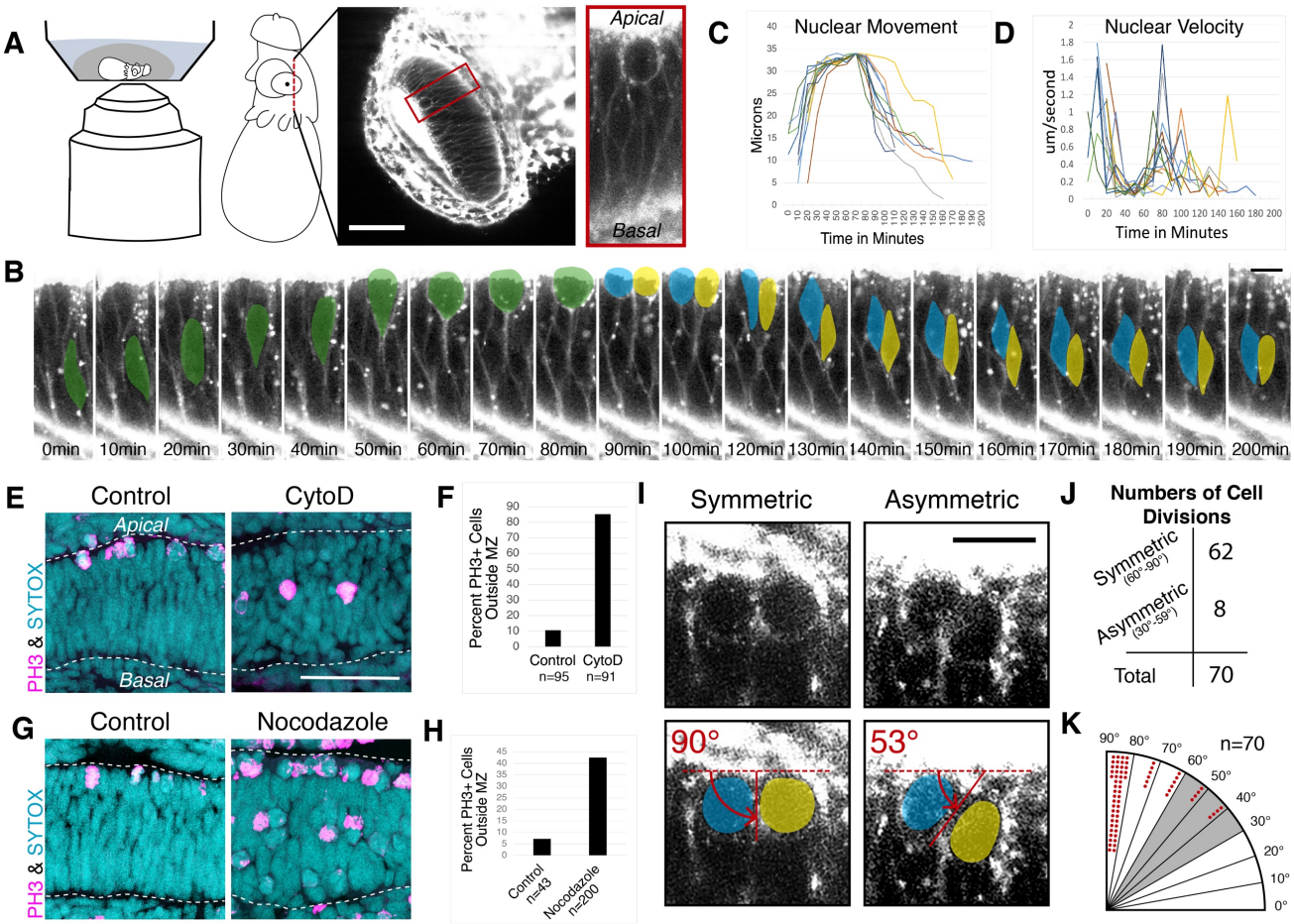

Figure 2: Nuclear migration and mitosis in the retinal epithelium. A. Schematic of squid embryo live-imaging. Scale is 50um **B.** False-colored timelapse of a single mitosis in the squid retina at stage 23 showing apical migration in the epithelium, mitosis, and basal migration. Apical is up, basal is down. Scale is 10um. **C.** Graph of nuclear movement as tracked using the Trackmate Fiji plugin (Schindelin et al., 2012). 13 nuclei tracked in 3 embryos. Tracks aligned to the highest point in migration. **D.** Graph of nuclear velocity calculated from the cells tracked in C. **E.** PH3 immunohistochemistry on actin polymerization inhibited squid retina at stage 23. 5uM Cytochalasin D and DMSO control treatment for 7 hours and immediate fix. Scale is 50um. **F.** Quantification of PH3+ nuclei outside the mitotic zone. **G.** PH3 immunohistochemistry on microtubule polymerization inhibited squid retina at stage 23. 5uM Nocodazole and DMSO control treatment for 7 hours and immediate fix. **H.** Quantification of PH3+ nuclei outside of the mitotic zone. **I.** Example of symmetric and asymmetric cell divisions observed in live-imaging experiments. Measurement of angle of division shown. Scale is 10um **J.** Quantification of symmetric (60°-90°) and asymmetric (30°-60°) cell divisions quantified from videos of 5 embryos and a total of 70 mitoses. **K.** Radial histogram quantification of division angles**.** Each dot represents a single mitosis.

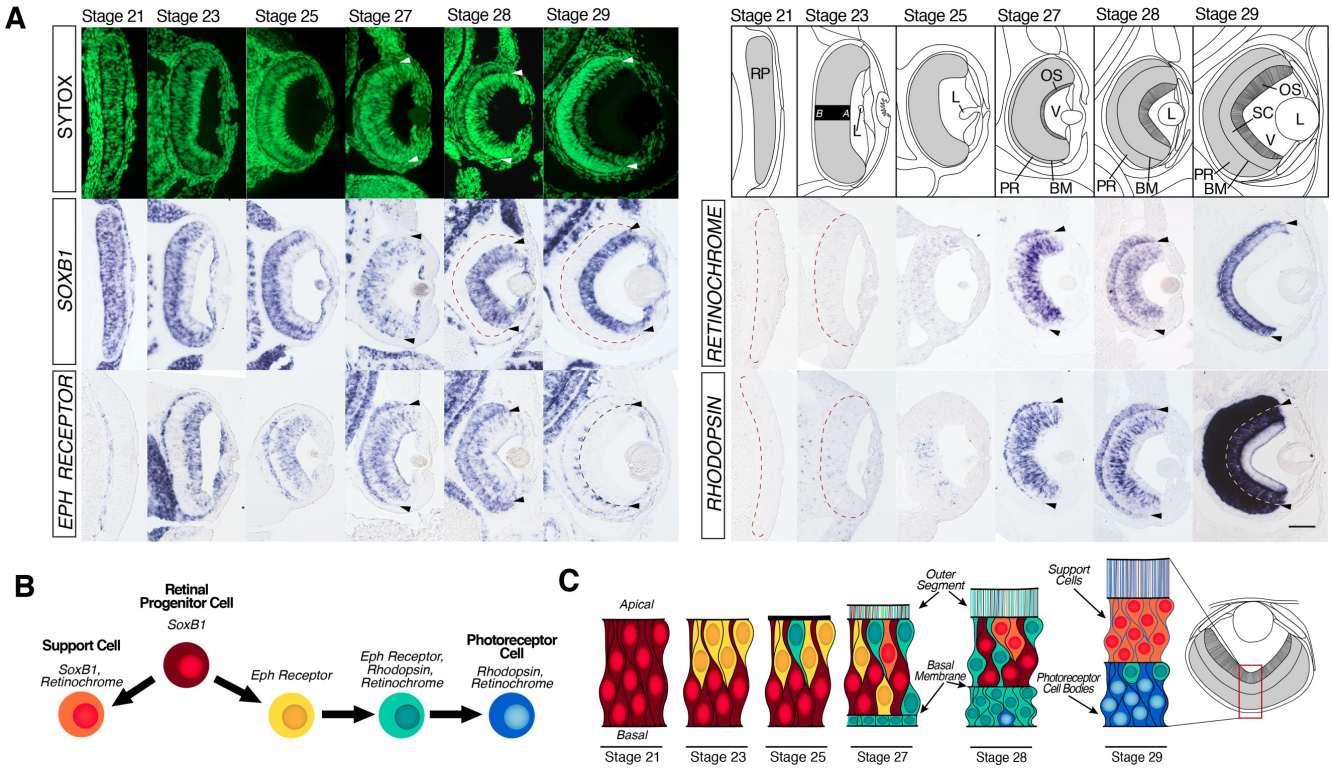

Figure 3: Molecular marker expression suggests a retinal differentiation trajectory. **A.** Staged mRNA expression in the developing cephalopod retina: *DpSoxB1, DpEphR, DpRhodopsin, DpRetinochrome*. Nuclear stain (sytox) shown in green. Schematic of stages labeled and shown. Arrowheads and black and white dotted lines identify the basal membrane. Red dotted lines identify the posterior retinal boundary. Scale is 50um. *RP,* Retinal Placode; *L* Lens; *OS,* Outer Segment; *BM,* Basal Membrane; *PR,* Photoreceptor Cells; *V,* Vitreous Space; *A,* Apical; *B,* Basal. Stage 21, 23, & 25 embryo anterior is down. Stage 27, 28, & 29 embryo dorsal is up. **B.** Hypothesis of cell differentiation trajectories. Color key is used in C. **C.** High magnification summary of time course gene expression data. At stage 21 the retina is homogenous. At stage 23 the retina is divided into apical and basal regions. At stage 25, evidence of terminal differentiation markers, *DpRhodopsin* and *DpRetinochrome*, are evident. At stage 27, the first nuclei are found behind the basal membrane and strict segregation of apical and basal expression is lost. Stage 28, the number of photoreceptor cells behind the basal membrane has increased and gene expression shows increased regional segregation. Stage 29, differentiation markers are robustly expressed.

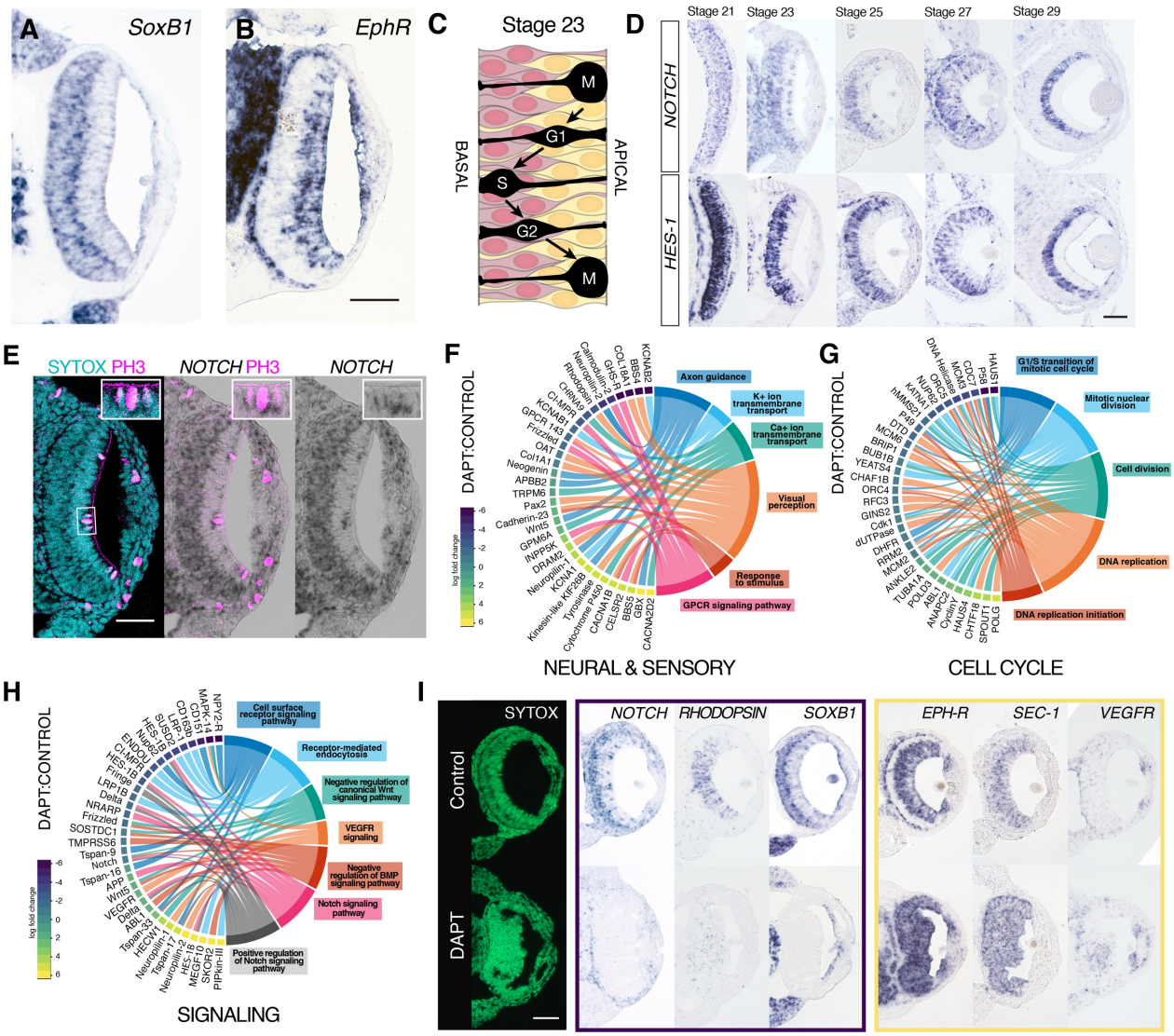

Figure 4: Notch signaling is required to maintain retinal pr-ogenitor cell identity. A. *DpSoxB1* expression on the basal side of the retina at stage 23 in retinal progenitor cells . **B.** *DpEphR* expression on the apical side of the retina at stage 23 in post-mitotic cells. Scale 50um. **C.** Schematic of nuclear migration within the pseudostratified retinal epithelium. Red (*DpSoxB1*) and yellow (*DpEphR*) color corresponds to gene expression and summary Figure 3B and 3C. **D.** *DpNotch* and *DpHes-1* expression correlates with *DpSoxB1* expression in the retinal progenitor cell population. Scale 50um **E.** *DpNotch* expression on the apical side of the retinal epithelium correlates with PH3 expression. Scale 50um. **F.** DAVID GO-annotations of RNA-seq results of Notch inhibited eyes. Embryos treated with 20uM DAPT and DMSO control at stage 23 for 24 hours. Eyes dissected for sequencing. All results shown have a p-value < 0.05. Neural sensory genes **G.** Cell-cycle genes **H.** Signaling pathway genes. Color Key is shared for all RNA-seq results. **I.** *In situ* hybridization on Control and Notch inhibited retina. Embryos treated with 20uM DAPT and DMSO control at stage 23 for 24 hours and fixed immediately. Nuclear stain (SYTOX-green) shown in green in the first column. Selected down-regulated genes in DAPT embryos in the purple box on the left. Selected up-regulated genes in DAPT embryos in the yellow box on the right. *DpSoxB1* expression, the retinal progenitor marker, is lost from the retina in Notch inhibited embryos. *DpEphR* expression, the neuroblast marker, has expanded expression throughout the retina in Notch inhibited embryos.